Teleimpedance Control of a Synergy-Driven Anthropomorphic Hand

A. Ajoudani, S. B. Godfrey, M. Catalano, G. Grioli, N. G. Tsagarakis and A. Bicchi

Abstract— In this paper, a novel synergy driven teleimpedance controller for the Pisa–IIT SoftHand is presented. Towards the development of an efficient, robust, and low-cost hand prothesis, the Pisa–IIT SoftHand is built on the motor control principle of synergies, through which the immense complexity of the hand is simplified into distinct motor patterns. As the SoftHand grasps, it follows a synergistic path with built-in flexibility to allow grasping of objects of various shapes using only a single motor. In this work, the hand grasping motion is regulated with an impedance controller which incorporates the user's postural and stiffness synergy profiles in realtime. In addition, a disturbance observer is realized which estimates the grasping contact force. The estimated force is then feedback to the user via a vibration motor. Grasp robustness and transparency improvements were evaluated on two healthy subjects while grasping different objects. Implementation of the proposed teleimpedance controller led to the execution of stable grasps by controlling the grasping forces, via modulation of hand compliance. In addition, utilization of the vibrotactile feedback resulted in reduced physical load on the user. While these results need to be validated with amputees, they provide evidence that a low-cost, robust hand employing hardware-based synergies is a viable alternative to traditional myoelectric prostheses.

I. INTRODUCTION

Although global amputation statistics are difficult to estimate, one in 200 people in the United States has lost a limb [1], whether due to trauma, disease, or war. Amputation requires an individual to adapt to significant physical and psychological loss in functional ability, independence, and appearance. Prostheses have been used for centuries to help restore function and cope with this loss. Body-powered prostheses saw great advancements in the middle of the last century and these hook-style prostheses are still often used today for their functionality, robust design, and modest sensory feedback. The next generation prosthetic devices are myoelectric: they are controlled using residual muscle signals and offer a more aesthetically pleasing appearance and can provide greater control of the hand.

The vast majority of myoelectrics are one degree of freedom (DOF) grippers with various levels of control complexity. Many offer basic on/off control for those with limited control over residual muscles. Others include proportional control by relating stronger electromyographic (EMG) signals to faster closing and/or higher grip force (eg: the Hosmer myoelectric hand by Centri or the Otto Bock DMC Plus®).

Authors are with the Dept. of Advanced Robotics, Istituto Italiano di Tecnologia, Via Morego 30, 16163, Genoa, Italy. A. Ajoudani, M. Catalano, G. Grioli, and A. Bicchi are also with the Centro di Ricerca "E. Piaggio", Universita di Pisa, 56126 Pisa, Italy. (e-mails: {arash.ajoudani, nikos.tsagarakis, sasha.godfrey}@iit.it, {manuel.catalano, giorgio.grioli, bicchi}@centropiaggio.unipi.it.

A few of these myoelectrics also feature anti-slip technology that automatically adjusts grip force upon detection of slippage (eg: the Otto Bock Sensor Hand^{TM}Speed). From these basic myoelectrics, there is a large gap in technology to the most advanced, and also most expensive, hands. These hands, including the i-limb^{TM}ultra from Touch Bionics, Inc and the Bebionic 3 from RSL Steeper, are anthropomorphic and are capable of adopting multiple realistic hand postures and grips. To accommodate the increased DOFs, however, the hands are more complex to control, often requiring sequential contractions or cocontractions to select and then operate a particular grip pattern.

In research, many solutions to the above challenges are being explored. For example, to allow more natural control of the prosthesis, complex machine learning algorithms are being employed [2], [3]. While capable of good classification in a lab setting, these methods are dependent on large training sets and few have been evaluated with day-to-day, real-world signal variation. In response to the difficulties faced in building and controlling anthropomorphic hands, the Pisa–IIT SoftHand [4] was developed as a joint venture between the Centro Piaggio of the University of Pisa and the Advanced Robotics Department of the Italian Institute of Technology. In the above machine learning examples, the burden of driving complex movement patterns falls on the controller. The SoftHand, however, shifts this burden to the hardware, with mechanics designed to follow natural paths. In order to control the many DOFs of the human hand, the brain builds sets of movement patterns, known as synergies [5], [6], [7], [8], thus the SoftHand was designed to actuate along the first synergy, with built-in compliance to allow for better molding to target objects. In addition to the basic position and force control currently available in prostheses, various features are being explored to increase ease of use and enhance the user's experience. Two of these features, that will be explored in this paper, are impedance control, which may provide more natural control of the hand [9], and vibrotactile feedback, which may minimize fatigue by allowing users to control the hand with less force [10].

With the goal of exploiting the efficiency and robustness of synergistic grasping, a novel myoelectric teleimpedance controller is developed. The concept of teleimpedance control has been previously presented as a practical approach for transferring human impedance-regulation skills and equilibrium position profiles to robots, in realtime. These previous works focused on impedance control in the proximal upper limb [11], [12] and lower limb [13]. In this work, an active impedance controller incorporating the user's hand stiffness and postural synergy profiles in realtime is presented. Exploi-

ting the concept of synergies that drive concurrent muscle activation, only one pair of antagonistic muscles (two EMG channels) was necessary for the musculoskeletal modeling of the grasp. The resultant model outputs were then used to command the stiffness and postural synergy references tracked by the developed impedance controller.

While visual feedback with a prosthesis can make up for some of the lack of proprioception, knowledge of task interaction forces is difficult to acquire. To that end, we developed a grasping contact force or finger interaction observer which incorporates the pre-identified disturbance model of the hand. Resulting interaction forces are then converted and applied to the user as vibrotactile feedback, providing real-time information on the contact forces in response to user-modified hand compliance and posture. The efficiency of the novel synergy-driven teleimpedance approach for dexterous manipulation has been evaluated through experiments with two subjects.

The rest of the paper is structured as follows: the SoftHand design considerations and the synergy reference models are described in sections II and III, respectively. Development of the interaction torque observer is discussed in section IV. The design of the teleimpedance controller is provided in section V, while experimental setup is presented in section VI. Results of the implementation of the novel synergy-based teleimpedance controller are shown in section VII. Finally, section VIII presents the conclusions.

II. THE PISA-IIT SOFTHAND

The Pisa-IIT SoftHand [4] was developed in a partnership between the Centro E. Piaggio of the University of Pisa and the Advanced Robotics department of the Italian Institute of Technology in Genoa, Italy. The goal was to build a robust and safe hand at low cost, while simplifying some of the immense complexity of the hand through the use of synergies. Two design strategies were combined to achieve this result: soft synergies and underactuation. As previously mentioned, synergies are a motor control strategy that coordinates the articulation of the many joints of the hand into coherent movement patterns. By incorporating synergies into the hardware design, there is a risk of poorly approximating the object to be grasped and providing uneven force at the contact points. In soft synergies, introduced in [8], the synergy serves as a reference position for a virtual hand, thus enabling better control of the interaction forces between the hand and the grasped object through variation of the virtual hand position or the stiffness matrix connecting the virtual and real hands. A fully actuated robotic hand (e.g. [14]) introduces one actuator per degree of freedom (DOF), thus increasing weight, cost, and control complexity of the final device. Underactuation [15], however, reduces the number of actuators without reducing the number of DOFs and also imparts a quality of shape adaptability to the device. These two strategies were combined to produce an "adaptive synergy" design strategy incorporating the neuroscientific basis of soft synergies with the shape adaptability of underactuation.

Using the adaptive synergy approach, an anthropomorphic hand was designed with 19 DOFs, 4 on each of 4 fingers, and 3 on the thumb. At rest, the hand measures roughly 23 cm from the tip of the thumb to the tip of the little finger, 23.5 cm from the wrist interface to the tip of the middle finger, and 4 cm thick at the palm. The fingers are capable of flexion/extension as well as ab/adduction. For ab/adduction of the fingers and at the equivalent of the carpometacarpal joint of the thumb (responsible for rotating the thumb from lateral pinch to C grasp, for example), traditional revolute joints were employed. One of the most important considerations in the design was safety: the hand must be robust enough to be of use to humans but also compliant enough to ensure safe interactions with humans. For this reason, a soft robotics approach was taken for the rest of the joints by incorporating rolling contact joints with elastic ligaments. The rolling contact joints ensure anatomically correct motion when actuated, but easily disengage on impact to allow safe interaction with humans while preserving the hand. The elastic ligaments also allow deformation while ensuring the hand returns to its original configuration. A single tendon runs through all joints to simultaneously flex and adduct the fingers upon actuation.

The hand is actuated by a single DC motor which moves the fingers on the path of the first synergy as described in [6] allowing the physical hand to mold around the desired object. The motor employed is a 6 Watt Maxon motor RE-max21 with an 84:1 gear reduction and a 12 bit magnetic encoder, resolution of 0.0875^o (Austrian Microsystems). With the current motor, maximum motor holding torque is 2 Nm and maximum holding force is roughly 20 N perpendicular to the palm.

III. SOFTHAND SYNERGY REFERENCES

Hand postural synergies have long been recognized as a motor control method to simplify hand complexity [5] and have been more recently broken down via principal component analysis to better understand this control strategy [6], [8]. Such patterns are deemed to be coded in the space of muscular activations [16], [17]. These observations promote the idea of exploring the minimum number of muscles necessary to decode and extract the information related to stiffness and equilibrium position references. In this work to estimate the required hand controller inputs and adopt the minimum required number of electromyography signals, we acquired and processed only one major antagonistic group of muscles acting on the hand. The extensor digitorum communis (EDC) and flexor digitorum superficialis (FDS) muscles are used in our experimental setup.

In order to map the EDC and FDS muscular activations to the stiffness and postural synergy commands in the most physiologically accurate way, a musculoskeletal model of the hand must be developed following procedures described in [18]. The musculotendon length and moment arm variations must be modeled as functions of finger movements along the first synergy. Eventually, parameters of the muscle model must be identified based on the user's physiological and

anatomical data. However, since the main application of the hand is for amputee use as a prosthesis, this parameter identification, if possible, will result in complex and invasive experiments. For this reason, here we propose a simpler and fairly reliable modeling of the SoftHand postural and stiffness synergy references.

To establish the mapping between the processed EMGs and the desired SoftHand postural and stiffness synergies, we used two single-neuron neural networks with the activation function of a modified hyperbolic tangent [19]. Therefore we can write:

$$q_s = \frac{a_q[1 - e^{-b_q(\text{FDS}-\text{EDC})}]}{[1 + e^{-b_q(\text{FDS}-\text{EDC})}]},$$

with a_q and b_q denoting constant gains which adjust the output range and the shape of the curve of the output, q_s, motor position synergy reference. FDS and EDC are the processed EMG signals of the corresponding muscles. Similarly for the stiffness:

$$K_s = \frac{a_k[1 - e^{-b_k(\text{FDS}+\text{EDC})}]}{[1 + e^{-b_k(\text{FDS}+\text{EDC})}]},$$

with a_k and b_k similar as above and K_s, denoting the stiffness synergy reference, is allocated in the stiffness interval of the robotic hand.

The parameters of the above mapping can be identified to relate the processed EMG signals to a desired position and stiffness interval of the corresponding device, eventually permitting the implementation of different control strategies including grasping motion assistance and/or hand/grasp stiffness control and augmentation. The realization of such control schemes could remarkably increase the efficiency of the SoftHand grasp for users with weak EMG signals, such as in amputees with muscle atrophy or short stump length.

To identify the parameters of the above single-neuron networks, subjects were asked to open and close the hand, trying to mimic the first synergy movement of the hand. As a reference, the SoftHand was slowly opened and closed. Meanwhile, FDS and EDC muscular activities were recorded. Subjects performed 20 grasping trials. Following that, subjects were asked to perform the grasp at 5 different FDS and EDC cocontraction levels. Visual feedback of the summated FDS and EDC levels was provided during the trial to assist the subjects in maintaining steady cocontraction levels. Four trials were recorded for each level, resulting in 20 trials in total. Eventually, parameter identification of the postural model (q_s) and stiffness model (K_s), and the corresponding motor position reference and SoftHand stiffness interval, respectively, was performed on even numbered trials while using FDS and EDC inputs. The bounds on the SoftHand stiffness parameter (outer controller loop gain, described below) were chosen experimentally, to balance the trade off between grasp compliance and good tracking performance. The odd numbered trials were used for the evaluation of the mappings. This led to the normalized root-mean-squared error (NRMSE) values of %16.4 and %11.8 for the postural and stiffness test trials, respectively, averaged across subjects.

IV. INTERACTION TORQUE OBSERVER

As mentioned previously, one DC motor is utilized to pull the tendon and drive the hand joints according to the first hand synergy. The equation of motor dynamics[1] is then defined by:

$$J_n\ddot{q} = K_{tn}I_{ref} - \tau_{dist}, \tag{1}$$

with $\ddot{q}$, K_{tn}, and I_{ref} denoting the motor angular acceleration, torque constant, and motor current, respectively. $J_n = J_m + \frac{J_h}{N^2}$ represents the total inertia (motor inertia plus hand intertia reflected to the motor side). In our setup, due to the low velocity profiles of the hand closure and the relatively high gear ratio, the reflected inertia of the hand, $\frac{J_h}{N^2}$, is neglected. The disturbance torque, τ_{dist}, combines all the internal and external disturbance torques and is assumed to be formed by four components: the elastic torque generated by the hand tendons during closure (τ_{te}), the gravitational effect (τ_{grav}), the frictional torque due to friction in the hand joints and pulleys (τ_f), and the interaction torque (τ_{int}). We can write:

$$\begin{aligned} \tau_{dist} &= \tau_{model} + \tau_{int} \\ &= \tau_{te} + \tau_f + \tau_{grav} + \tau_{int}. \end{aligned} \tag{2}$$

In the above equation, due to the lightweight design of the hand, the effect of gravitational torque is neglected. The hand closure elastic torque component is modelled as a function of the motor shaft rotation angle. In addition, an antisymmetric piecewise-linear function of the motor speed and tendon tension is used to model the viscous and Coulomb friction of the hand [20], as follows,

$$\tau_f(\dot{q}) = \begin{cases} D_1\dot{q} + n_{s_1}K_{te}(q - q_o) & \dot{q} > 0 \\ D_2\dot{q} - n_{s_2}K_{te}(q - q_o) & \dot{q} < 0, \end{cases} \tag{3}$$

with D_i, n_{s_i}, K_{te}, and q_o representing the viscous damping and Coulomb friction coefficients, the reflected hand tendon stiffness, and motor angular position at rest (hand open), respectively. Incorporating the above assumptions in the disturbance model of the hand will result in:

$$\tau_{model_i} = (1 + n_{s_i})K_{te}(q - q_o) + D_i\dot{q}, \tag{4}$$

with the index i referring to the antisymmetric Coulomb and velocity dependent components of the friction model. Therefore, the hand closure and opening models will be identified separately, as described below.

Supposing that the hand has not come in contact with the object to be grasped (i.e. $\tau_{int} = 0$ in eq. 2), the hand model torque (τ_{model}) can be computed from the motor current and its motion response. Such calculation would require motor current and acceleration sensing with the latter being sensitive to noise if computed from position differentiation. To achieve reliable hand model torque estimation while taking into account the minimum hardware requirements, a robust torque observation technique is used here. In particular, the

---

[1]In this paper, if not stated explicitly, all the variables and equations are described on the motor side (including interaction torque). Therefore, a gearbox ratio of $N = 84$ must be taken into account for the presentation of the variables after the gearbox.
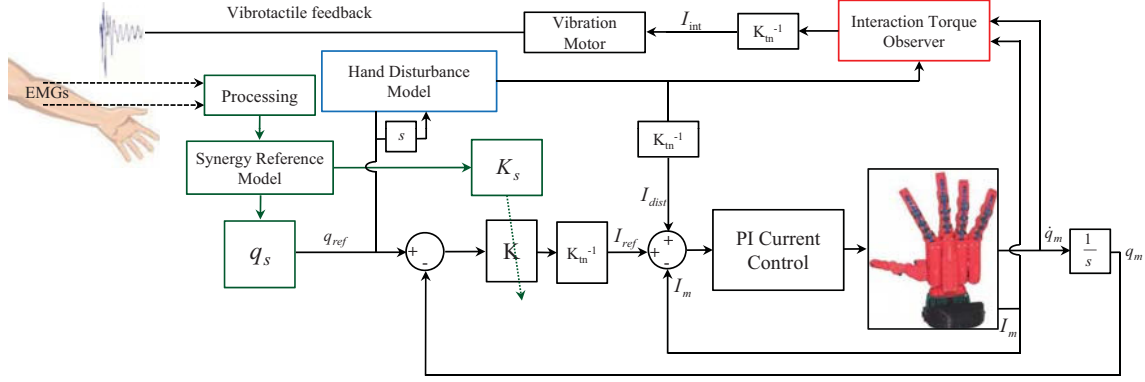
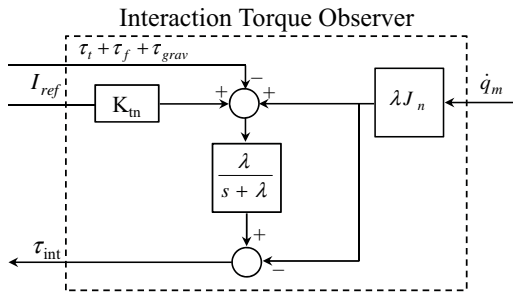**Fig. 1:** Block diagram of the synergy-driven hand teleimpedance.

Fig. 2: Interaction torque observer block diagram.

hand model torque is estimated based on the angular velocity as follows:

$$\widehat{\tau}_{model} = K_{tn}I_{ref} - J_n\ddot{q}$$
$$= \frac{\lambda}{s+\lambda}(K_{tn}I_{ref} - J_n s\dot{q}) \qquad (5)$$
$$= \frac{\lambda}{s+\lambda}(K_{tn}I_{ref} + \lambda J_n\dot{q}) - \lambda J_n\dot{q}.$$

Here, s is the Laplace operator and λ represents the filter cutoff frequency which affects the disturbance rejection capability [21]. The major design criterion is to choose λ low enough to result in a robust system, while considering the introduced filtering delay. Now, to estimate the reflected interaction torque caused by the contact of the hand with the environment, we take equations (1) and (5) into account and subtract the identified hand model torque (equation (4)), from the external torque effect as follows:

$$\widehat{\tau}_{int} = \frac{\lambda}{s+\lambda}(K_{tn}I_{ref} + \lambda J_n\dot{q} - \widehat{\tau}_{model}) - \lambda J_n\dot{q}. \qquad (6)$$

The block diagram of the interaction torque observer is shown in figure (2). To identify the parameters of the hand model (equation (4)), the hand controller was driven with low velocity (quasi-static) reference trajectories. Such motion reference profiles were designed to result in complete hand closure, starting from fully extended fingers. This process was repeated in the reverse direction to identify the model parameters for the opening of the hand. The antisymmetric and velocity dependent properties of the friction model were

the main reasons for separate identification of the hand closure and opening models.

Consequently, the resultant current, position, and velocity profiles were used to estimate the components of the equation (4), by means of conventional least squares identification algorithm. The identification process led to two feed-forward, velocity dependent estimates of the hand disturbance model, $\widehat{\tau}_{model}$.

V. CONTROLLER DESIGN

The wearable prosthetic hand in contact with the human forms a local master-slave system, the efficiency of which is partially governed by the proper transmission of the signals (force, position, velocity and etc) between the two. As an alternative solution to the EMG based classical control of the prosthetic/robotic hand [9], [22], our proposed teleimpedance controller incorporates the user's position and stiffness synergy profiles in the control of a soft and robust grasp. The overall block diagram of the proposed controller is shown in figure (1). In this control scheme, the inner loop is a high bandwidth current regulator while the outer loop implements a position controller which incorporates a time varying gain and is updated by the user's hand stiffness synergy profile in realtime. This value is adjusted by the realtime stiffness synergy model developed in section III. The lower bound of the stiffness gain was experimentally chosen to guarantee good tracking performance as well as high grasp compliance. Simultaneously, acquired muscular activities were used to determine reference position profiles as described earlier in section III.

The hand disturbance model block estimates the hand model torque, relying on previously developed and identified feed-forward models (equation 4). The estimated torque is then converted to the current and fed to the inner current controller as I_{dist}. In the meantime, the estimated hand model torque is used by the interaction torque observer (figure 2), to estimate the interaction torques due to contact with the grasped object. Subsequently, the resulting interaction torque is converted and applied to the vibration motor in order to provide the user with some indication of the grasp state and

force. Smooth and skillful grasp control can be achieved by the user with the modulation of the interaction forces by means of controlling the hand compliance.

VI. EXPERIMENTAL SETUP

Analog electromyography signals were measured and amplified with a Delsys-Bangoli 16 (Delsys Inc.) apparatus. Acquired signals were band-pass filtered within the 20-450 Hz frequency range. Resulting signals were sampled at 2 kHz (PCI-6220, National Instruments) and full rectified for further processing. A digital, non-causal FIR linear phase low-pass filter was used for the detection of the envelope of the signal, which approximately corresponds to muscle activity. EMG normalization was performed automatically. Each time the system was activated, subjects were given 5 seconds to perform maximal cocontactions. This input was then used to normalize the EMG signals online. The normalized signals were fed into the model described in section III.

The hand unit controller and power driver for the motor are custom control boards based on the Texas Instruments Luminary DSP chip LM3S8962. The DSP control loop is executed at 1KHz while the communication with the host PC is achieved through a real time Ethernet link. Motor current measurement is performed by a hall effect based current sensor (ACS714, Allegro Microsystems Inc.) and appropriate signal conditioning integrated in the motor power driver module.

A small (24 × 7 mm), low-cost eccentric mass motor (Precision Microdrives™) was utilized to provide the user with vibrotactile feedback. To that end, the observed interaction torque was experimentally scaled and fit to the input voltage range of the vibration motor. A USB-6009, National Instruments board was employed to apply the desired analog voltage to the actuator. The actuator was placed on the back of the hand to minimize the effect of applied vibrations on EMG signal acquisition.

The data acquisition and synchronization interfaces between the motor controller board, the interaction torque observer, the hand model torque, the EMG acquisition board, the hand musculoskeletal model, and the vibration motor were developed in C++. The acquisition, processing and control ran at 1KHz sampling frequency.

Experiments were designed to evaluate the effectiveness of vibrotactile feedback and user-modified compliance in controlling the natural, robust grasp of the SoftHand. For this reason, objects with different elastic properties were grasped under the following hand controller parameters: i) fixed and relatively high stiffness gain (Stiff), ii) fixed and relatively low stiffness gain (Compliant), and iii) user modified hand compliance (Teleimpedance), all with or without the effect of vibrotactile feedback. Postural synergy commands were derived from the model, described in section III, and were consistent among all experiments. Subjects stood in front of a table and reached to an object. Successful grasp was achieved when the SoftHand held the object securely off the surface of the table. Each grasp was attempted 3 times. Before the

experiments, subjects were provided with adequate training trials to minimize the learning effect.

VII. RESULTS

A. Interaction Torque Observer

In order to validate the accuracy of the identified hand model, the hand controller was provided with a sine wave position trajectory. The trajectory led to the execution of four SoftHand half-closure and full-opening movements. A soft, deformable ball was grasped during the second and third closures and removed on the first and the last. By pre-determined placement of the soft obstacle along the hand closure, the hand molded around the obstacle with two (figure 4-c_1) or three fingers (figure 4-c_2) contacting the object, causing small deformations on the ball's surface. The motor current (I_{ext}) was measured and used for the detection of contact and estimation of the interaction torque during the grasping of the ball.
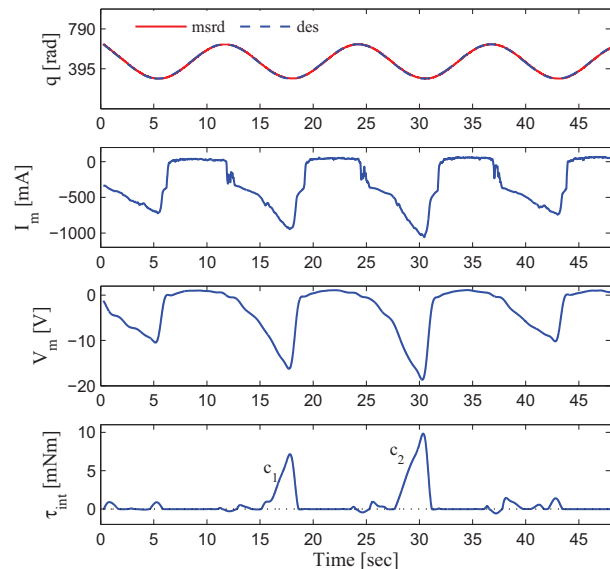

Fig. 3: Results of a grasping experiment with fixed stiffness gain. A soft, deformable ball was used as an object to grasp during the second and third closures and removed on the first and the last. The top three plots demonstrate the position tracking, motor current and motor voltage profiles, from the top down. Observed interaction torques once the soft obstacle was squeezed by two (c_1) or three (c_2) fingers are provided in the bottom plot.

Figure (3), illustrates the results of this experiment. The top three plots demonstrate the position tracking, motor current, and motor voltage profiles, from the top down. Observed interaction torques once the soft obstacle was squeezed by two (c_1) or three (c_2) fingers are provided in the bottom plot. During the first and last closures, the fingers did not contact the object, resulting in low interaction torques. In addition, although a soft and deformable obstacle was grasped by only two or three fingers, interaction torque fluctuations were efficiently monitored.
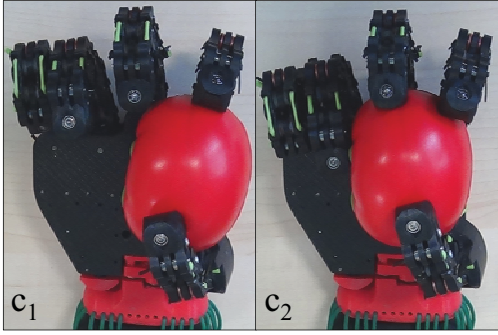
Fig. 4: The SoftHand molds around the obstacle using two (c_1) or three (c_2) fingers, during grasping.

B. Grasping Experiments

Subjects were able to grasp objects with different elastic properties when the SoftHand was provided with Teleimpedance or Stiff controllers (see section VI for details of the setup). However, the Stiff controller caused undesired deformations in the surface of soft objects. These deformations were not observed in the experiments using the Teleimpedance or Compliant controllers. In the latter, subjects were able to shape the SoftHand around all objects, but were unable to lift heavy and low-friction objects (e.g. mug and ball) due to low levels of hand force resulting in object slippage on lift. Nevertheless, it is worth noting that, since the motor is provided with the estimated hand disturbance current (I_{dist}, see figure 1), fairly good tracking is achieved even when the SoftHand is operated under the Compliant controller.

Typical results of an experiment, in which the subject grasped a rigid object (mug) are illustrated in figure 5. Here, the SoftHand was executed under Stiff (5.a), Compliant (5.b) and Teleimpedance (5.c) controllers. The top and middle plots contain the desired and measured postural synergy references (upper portion of each) and the observed interaction torques between the hand and the grasped object (lower portion of each) for Stiff and Compliant controllers, respectively. The third plot, fig. (5.c), illustrates the postural references, interaction torques, and subject's muscular activities while using Teleimpedance control. The stiffness synergy reference, K_s, as a result of subject cocontractions is normalized to the chosen maximum stiffness gain (50 Nm/rad) and depicted in the bottommost portion of fig. (5.c).

As shown in the plots, high interaction forces are realized once the grasp is executed with the Stiff controller under high, fixed gain. Such behavior is not desirable when grasping fragile or soft objects and can cause damage or deformation, either to the object or the prothesis itself. In addition, abrupt changes of the interaction forces are seen due to the rigidity of the hand. On the other hand, the Compliant controller with reduced stiffness gain produced lower interaction forces but was unable to provide the task forces required to complete the task.

Unlike in the Complaint and Stiff cases, user-modified compliance of the hand used in Teleimpedance control, together with the postural synergy profiles, provide the possibility
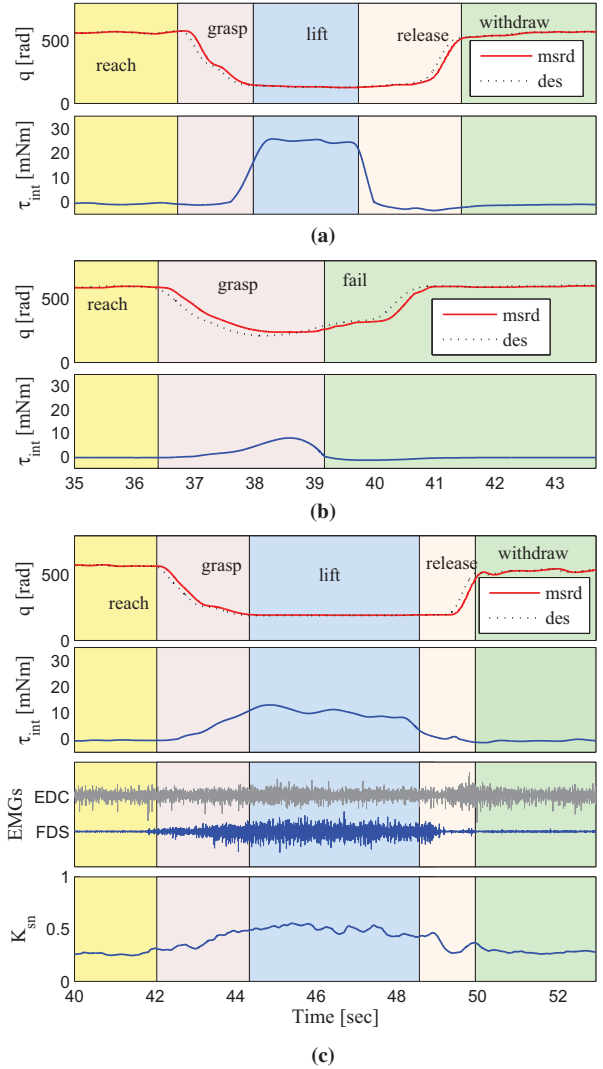

Fig. 5: Experimental results of the SoftHand grasping a hard object (mug), with the controller under a) high, fixed stiffness gain (K= 40 Nm/rad), b) low, fixed stiffness gain (K= 10 Nm/rad), and c) teleimpedance ($a_q = 1$, $b_q = 5.03$, $a_k = 1.87$, and $b_k = 0.579$, for this subject).

of adjusting task-related grasp forces (figure 5.c). With this controller, lower cocontractions resulted in high compliance, allowing gentle grasping of fragile or deformable objects, while higher stiffness values were generated with higher cocontractions to grasp heavier or more rigid objects. This feature enables smooth modulations of the hand forces, in contrast with the Stiff controller, while still allowing task completion. The SoftHand teleimpedance controller was also tested with activities of daily living (e.g. opening and closing a jar lid, etc). A video of the experiment is available at [23]. In figure (6), a subject used the SoftHand to demonstrate the steps to make an espresso.

The effect of vibrotactile feedback on muscular activity levels was tested on one subject; this feedback resulted in lower muscular activity levels in Teleimpedance and Stiff controllers. Muscular activities were averaged across all trials either with or without feedback (grasping objects

Fig. 6: SoftHand making an espresso.

with different elastic properties) for a given control scheme. The reduction ($\approx \%10$) in the average EMG levels with vibrotatile feedback, suggests a reduction in the subject's physiological load. As in the other grasping experiments, the effect of vibrotactile feedback was tested following adequate familiarization of the subject with the device and the controller.

VIII. Conclusions

In this paper, a novel synergy-based teleimpedance controller was developed to gather the user's postural and stiffness synergy references from two EMG channels. Two single-neuron networks were utilized in order to establish the mapping between the EMGs and the postural and stiffness synergies. Resulting synergy commands were then tracked by the developed SoftHand controller in realtime. The controller provided the user with the possibility of modifying the compliance of the grasp, via cocontractions. In addition, a torque observer was developed in order to monitor the interaction forces between the grasped object and the hand. Observed torque was then converted and applied to the user via an eccentric mass motor. The efficiency of the novel synergy-driven teleimpedance controller for dexterous manipulation was evaluated through experiments with two subjects. Incorporation of the above features resulted in robust and reliable grasps, regardless of the elastic properties of the grasped object.

IX. Acknowledgements

References

[1] NLLIC Staff, "Amputation statistics by cause, limb loss in the united states," *National Limb Loss Information Center, Knoxville, TN*, 2008.

[2] N. Jiang, K. Englehart, and P. Parker, "Extracting simultaneous and proportional neural control information for multiple-dof prostheses from the surface electromyographic signal," *Biomedical Engineering, IEEE Transactions on*, vol. 56, no. 4, pp. 1070–1080, 2009.

[3] D. Naidu, C. Chen, A. Perez, and M. Schoen, "Control strategies for smart prosthetic hand technology: An overview," in *Engineering in Medicine and Biology Society, EMBS 2008*.

[4] M. G. Catalano, G. Grioli, A. Serio, E. Farnioli, C. Piazza, and A. Bicchi, "Adaptive synergies for a humanoid robot hand," in *IEEE-RAS International Conference on Humanoid Robots*, 2012.

[5] M. A. Arbib, "Coordinated control programs for movements of the hand," *Hand function and the neocortex*, pp. 111–129, 1985.

[6] M. Santello, M. Flanders, and J. Soechting, "Postural hand synergies for tool use," *The Journal of Neuroscience*, vol. 18, no. 23, pp. 10 105–10 115, 1998.

[7] M. Gabiccini, A. Bicchi, D. Prattichizzo, and M. Malvezzi, "On the role of hand synergies in the optimal choice of grasping forces," *Autonomous Robots*, vol. 31, no. 2, pp. 235–252, 2011.

[8] A. Bicchi, M. Gabiccini, and M. Santello, "Modelling natural and artificial hands with synergies," *Philosophical Transactions of the Royal Society B: Biological Sciences*, vol. 366, no. 1581, pp. 3153–3161, 2011.

[9] T. Tsuji, O. Fukuda, H. Shigeyoshi, and M. Kaneko, "Bio-mimetic impedance control of an emg-controlled prosthetic hand," in *Intelligent Robots and Systems,(IROS 2000)*. IEEE.

[10] C. Pylatiuk, A. Kargov, and S. Schulz, "Design and evaluation of a low-cost force feedback system for myoelectric prosthetic hands," *JPO: Journal of Prosthetics and Orthotics*, vol. 18, no. 2, p. 57, 2006.

[11] A. Ajoudani, N. Tsagarakis, and A. Bicchi, "Tele-Impedance: Teleoperation with impedance regulation using a body-machine interface," *International Journal of Robotics Research*, vol. 31(13), pp. 1642–1655, 2012, http://www.youtube.com/watch?v=KPO6IO7Tr-Q.

[12] A. Ajoudani, M. Gabiccini, N. G. Tsagarakis, A. Albu-Schäffer, and A. Bicchi, "TeleImpedance: Exploring the role of common-mode and configuration-dependant stiffness," in *IEEE International Conference on Humanoid Robots*, 2012.

[13] N. Karavas, A. Ajoudani, N. G. Tsagarakis, J. Saglia, A. Bicchi, and D. G. Caldwell, "Tele–impedance based stiffness and motion augmentation for a knee exoskeleton device," in *IEEE International Conference on Robotics and Automation (ICRA2013)*, 2013.

[14] F. Lotti, P. Tiezzi, G. Vassura, L. Biagiotti, and C. Melchiorri, "Ubh 3: an anthropomorphic hand with simplified endo-skeletal structure and soft continuous fingerpads," in *IEEE Conf. Robotics and Automation, ICRA 2004*.

[15] L. Birglen, C. Gosselin, and T. Laliberté, *Underactuated robotic hands*. Springer Verlag, 2008, vol. 40.

[16] W. Lee, "Neuromotor synergies as a basis for coordinated intentional action," *Journal of Motor Behavior*, vol. 16, no. 2, pp. 135–170, 1984.

[17] P. K. Artemiadis and K. J. Kyriakopoulos, "Emg-based control of a robot arm using low-dimensional embeddings," *Robotics, IEEE Transactions on*, vol. 26, no. 2, pp. 393–398, 2010.

[18] T. Buchanan, D. Lloyd, K. Manal, and T. Besier, "Neuromusculoskeletal modeling: estimation of muscle forces and joint moments and movements from measurements of neural command," *Journal of applied biomechanics*, vol. 20, no. 4, p. 367, 2004.

[19] C.-T. Chen and W.-D. Chang, "A feedforward neural network with function shape autotuning," *Neural networks*, vol. 9, no. 4, pp. 627–641, 1996.

[20] C. C. De Wit and P. Lischinsky, "Adaptive friction compensation with partially known dynamic friction model," *International journal of adaptive control and signal processing*, vol. 11, no. 1, pp. 65–80, 1997.

[21] T. Murakami, F. Yu, and K. Ohnishi, "Torque sensorless control in multidegree-of-freedom manipulator," *Industrial Electronics, IEEE Transactions on*, vol. 40, no. 2, pp. 259–265, 1993.

[22] C. Cipriani, F. Zaccone, S. Micera, and M. C. Carrozza, "On the shared control of an emg-controlled prosthetic hand: analysis of user–prosthesis interaction," *Robotics, IEEE Transactions on*, vol. 24, no. 1, pp. 170–184, 2008.

[23] Video, http://www.youtube.com/watch?v=vByEmyABu3E.